Nuclear Instruments and Methods in Physics Research A245 (1986) 248–261
North-Holland, Amsterdam

HERA VARIABLE-ENERGY "MINI" SPIN ROTATOR AND HEAD-ON ep COLLISION SCHEME WITH CHOICE OF ELECTRON HELICITY

Jean BUON

Laboratoire de l'Accélérateur Linéaire, Orsay, France

Klaus STEFFEN

Deutsches Elektronen-Synchrotron DESY, Hamburg, FRG

Received 27 November 1985

The novel scheme of spin rotation and head-on collision in the HERA electron–proton collider is described with emphasis on the means for obtaining a high degree of longitudinal electron polarization of either sign at the interaction points. The variable-energy "mini" rotator employed in this scheme is described and discussed, and also the depolarizing effect of radiative spin diffusion and the means to counteract it. The designed scheme covers the whole range of electron energies between 27 and 35 GeV, with a maximum degree of Sokolov–Ternov polarization of 84% at 35 GeV.

1. Introduction

In HERA, the electron–proton storage ring facility under construction at DESY in Hamburg [1], 820 GeV protons will collide with 30 GeV electrons at four interaction points. The proton ring, employing superconducting bending and focusing magnets, will be housed on top of the electron ring in a 6.3 km long underground ring tunnel. The two beams, each consisting of 200 particle bunches, will collide head-on in the middle of four 360 m long straight sections. Originally, the beams were planned to cross at an angle of 20 mrad at the collision point. Calculations, however, emphasized the danger of synchro-betatron resonances excited by the finite crossing angle [2] and led to designing and adopting a collinear collision scheme [3–5].

A high degree of longitudinal polarization in the colliding electron beam is a fundamental claim of the HERA proposal. In the arcs of the ring, the emission of synchrotron radiation in the bending magnets aligns the electron spin in the vertical direction, antiparallel to the field (Sokolov–Ternov effect [6]). In order to have it longitudinal at interaction, a pair of 90° spin rotators must be installed around each interaction region which turns the spin, after leaving the arc, into the beam direction and then back into the vertical again before entering the following arc.

Various types of spin rotators were investigated and discarded again, employing either transverse field magnets alone [7], or combined with a very strong superconducting solenoid [8]. The latter, although in principle offering a high degree of polarization, has the practical handicap of requiring a space-consuming fully antisymmetric geometry in order to work in a finite energy range. The type that survived is the so-called "mini rotator" [7,9], with small integral field and small vertical beam excursion. In its present form, after going through various stages of improvement [10–12], it allows to have either sign of electron helicity, i.e. to invert the longitudinal spin direction, and works at any energy between about 27 and 35 GeV.

Rotators, when inserted, will in general destroy the "spin transparency" of the ring, which means that the quantum emissions will cause a diffusion of the spin and thus a depolarization of the electron beam. However, by properly adjusting the optics, the spin transparency can be restored [13,14].

A satisfactory spin-transparent setup with mini rotators was initially designed for the 20 mrad crossing angle geometry [9,15]. It has been adapted afterwards to head-on interaction [3] by splitting up the rotator magnet nearest to the interaction point and employing part of it to separate the electron beam from the proton beam near the interaction point. This shifted the interaction point laterally and created a spin transparency problem which was subsequently overcome by adding an extra pair of beam translation magnets between rotators [16]. A fully spin-transparent optics, with four pairs of mini rotators, is available [17] and permits a polarization of 84% at 35 GeV in the undistorted machine.

In practice, of course, the machine will always be

0168-9002/86/$03.50

distorted by field and alignment errors, but the depolarizing effect of these errors can be substantially reduced by employing the method of "harmonic spin matching" to the three modes of oscillations excited by radiation [18–20]. For horizontal oscillations this was experimentally demonstrated in PETRA [18]. The most efficient reduction is required in the upper part of the energy range, where the increased energy spread in the beam enhances the depolarization [21].

2. Mini rotator concept

If, in a transverse magnetic field, the beam direction is rotated by an angle ϕ, the spin of on-momentum particles is rotated about the same axis by an angle

$$\psi = \nu\phi$$

in the coordinate system following the beam direction (orbit frame). The factor ν is the product of the Lorentz factor γ and the gyromagnetic anomaly a, given numerically for electrons by

$$\nu = \gamma a = \frac{E[\mathrm{GeV}]}{0.44065}.$$

Around the closed orbit of a planar storage ring, with $\phi = 2\pi$, ν is the number of spin precessions per revolution and is called the spin tune.

With this relation, a great variety of rotators may be composed of horizontal and vertical bending magnets [7], rotating the spin from the vertical into the longitudinal direction, as required. Among this variety the mini rotator is the most favourable for HERA [9].

It derives, in principle, from a so-called "Siberian Snake" that was found several years ago [22], where each half-snake consists of six bending magnets that produce a vertical and a horizontal matched beam bump which are folded into each other and start and end with a 45° spin rotation each (see fig. 1). This half-snake would rotate the spin by 90° about the longitudinal axis (snake of first kind). It transforms into the rotator by inverting the sign of the last bending magnet; this changes the outgoing spin orientation by $2 \times 45°$ and makes it come out longitudinal instead of transverse horizontal. The rotator, then, is not a straight unit as the snake was, but bends the beam in the horizontal plane by an angle corresponding to 90° spin rotation. This bend can be incorporated into the arc of the ring by making the rotators an integral part of it. A pair of such mini rotators is symmetric in the horizontal plane with respect to the interaction point, but antisymmetric in the vertical plane.

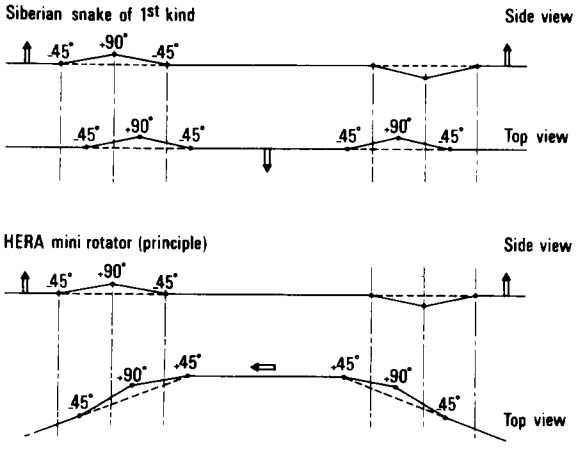

Fig. 1. Sketch of the principle of mini rotator pair as obtained from a Siberian Snake of the first kind (spin rotations in degrees; arrows indicate spin direction).

In practice, the spin rotation angles in the mini rotator may be taken different from this basic scheme; for a given overall geometry, there still is a multidimensional variety to be chosen from. The relevant rotator properties within this variety are surveyed in sect. 4.

3. Energy variation of mini rotator

The rotator is laid out for a chosen design energy at which it simultaneously provides the correct beam geometry and spin rotation. For given magnet strength, the beam deflection varies inversely with energy, while the spin rotation in the orbit frame is independent of energy. Therefore, when varying the beam energy one cannot maintain the beam geometry and the individual spin rotations at the same time. If the horizontal beam geometry is maintained by ramping the horizontal rotator magnets with energy, in synchronism with all other ring magnets, then the vertical beam geometry must be changed in order to keep the spin direction vertical in the arcs, an essential requirement to avoid large depolarization. This can be done by adjusting the amplitude of the vertical beam bump [7]. The rotator can thus be operated in a range of plus or minus a few percent about its design energy, as had been initially proposed to provide the flexibility needed in tuning the ring for maximum polarization.

There remained, however, the question of where to fix the design energy of the rotator. Initially, it was set at 27.5 GeV, the maximum energy that can be reached in the HERA electron ring with its initial outfit of rf transmitters and cavities taken from the existing 23 GeV storage ring PETRA, which will then solely be used as a HERA injector. However, physics interest asks for the highest possible electron energy, and an increase in top energy is foreseen by installing superconducting rf cavities in the electron ring at some time. Moreover, the increase of energy up to, say, 35 GeV has the advantage of reducing the polarization time from 40

to 12 min and also to increase by several percent the maximum degree of Sokolov–Ternov polarization (see fig. 6).

The range of energy from 27 to 35 GeV cannot be covered by tuning only the vertical beam bump. Instead, it has been found that the energy of the rotator can quite effectively be varied within this whole range by varying a small horizontal beam bump [23,10], superimposed on the rotator, together with the vertical beam bump. This feature not only allows to maintain the vertical spin direction in the arcs, but also the longitudinal spin direction at the interaction point. Such a variable horizontal beam bump is incorporated in the present design of the mini rotator [12].

4. Properties and survey of mini rotators

In the vertical plane, a pair of mini rotators must be antisymmetric with respect to its center. In the horizontal plane, however, the pair may either be symmetric or antisymmetric. The properties of these two types [24] are subsequently compared.

Fully antisymmetric rotator pairs have the basic advantage that antisymmetric error configurations have no effect on the spin transformation. In particular, such rotators will work over a large energy range at constant beam geometry, and the effect of systematic magnet errors will cancel as well. This is nice, but makes it difficult to devise orthogonal controls for the outgoing spin direction [23].

Horizontally symmetric mini rotators, on the other hand, contribute to the horizontal bending of the beam in the ring. They replace some normal bending magnets. This feature gives some space for rotator installation which otherwise would be difficult to provide in a ring like HERA.

Moreover, the degree of polarization allowed by the Sokolov–Ternov effect is larger for horizontally symmetric pairs of rotators composed of bending magnets than for antisymmetric pairs. The degree P of polarization is approximately given by

$$P = P_0 \frac{1 + \sum_i \left(\frac{\rho_0}{\rho_i}\right)^2 \frac{|\phi_i|}{2\pi} \cos\theta_i}{1 + \sum_i \left(\frac{\rho_0}{\rho_i}\right)^2 \frac{|\phi_i|}{2\pi}} \qquad (1)$$

$(P_0 = 92.376\%)$,

where ρ_0 and ρ_i are, respectively, the bending radii in the normal arc magnets and in the ith rotator magnet, and ϕ_i is the beam line rotation produced by this rotator magnet. The angle θ_i is the angle between the magnetic field and the polarization direction in this magnet ($\theta_i = 0$ for the direction antiparallel to the field). The numerator of this formula shows the contribution of each magnet to the Sokolov–Ternov polarizing effect, which changes sign if the field is reversed. On the other hand, the denominator gives a depolarizing effect independent of the direction of the field.

In horizontally symmetric pairs of rotators, the horizontally bending magnets contribute globally to polarize the beam by the Sokolov–Ternov effect, even if one of them bends in the oppposite direction. On the other hand, if in a fully antisymmetric pair of rotators one horizontally bending magnet bends in the normal direction, then the corresponding magnet in the other rotator of the pair bends in the opposite direction. Their polarization effects cancel out, while their depolarizing effects add together. This feature is exactly the cancellation of the $\cos\theta_i$ terms in the numerator of the above formula. The result is a lower maximum polarization than for horizontally symmetric pairs of rotators.

However, horizontally symmetric rotator pairs have, in general, the disadvantage of producing a spin tune shift [7]. Although, after passing through such a pair, the equilibrium spin direction is restored, the spin precession phase is modified as compared to the ring without rotators, leading to a variation of the total spin precession per turn, i.e. a spin tune shift. As a result of the energy tuning of the vertical and horizontal beam bumps in the mini rotators, the spin tune shift also varies with energy. On the contrary, the spin transfer matrix through a fully antisymmetric pair of rotators is exactly unity at any energy; therefore there is no spin tune shift.

Normally, the beam energy is set such that the spin tune is near to half-integer, i.e. as far away as possible from linear depolarizing resonances which occur when the spin tune fulfills the general relation

$$\nu = n \pm n_z Q_z \pm n_x Q_x \pm n_s Q_s,$$

where n is an integer and $n_{z,x,s} = 0, 1$. When turning the mini rotators on, the spin tune shift must be sufficiently small to not approach any depolarizing resonance; otherwise the beam energy will have to be slightly varied for compensating this shift.

The most important property characterising a rotator is its effect on maximum polarization. In a flat ring, the upper limit for Sokolov–Ternov polarization is $8/(5\sqrt{3}) \approx 92.4\%$. In a ring with rotators this upper limit is decreased as the polarization vector does not coincide with the magnetic field direction in all the rotator magnets. According to eq. (1), the reduction in polarization $\Delta P/P$ goes with the square of the bending strength in these magnets and can thus be reduced by making the magnets weaker and longer. As the total length of the rotator is restricted by other considerations, like ring geometry, different rotators should be compared at a given total length L. A figure of (anti-)merit for any rotator is given by the product $L^2 \Delta P/P$.

Besides the limitation in ring space available for inserting the rotators, their length is also restricted by the possible transverse beam excursion in the rotator and by the focusing needed to limit transverse beam dimensions.

The transverse beam excursion is given by the amplitudes of the vertical and horizontal beam bumps. This excursion is directly proportional to the rotator length. In the HERA mini rotator, the vertical excursion is less than ± 22 cm (both signs needed for inverting helicity), and the total horizontal excursion is 19 cm in the 27–35 GeV energy range.

The chosen relatively small length of the mini rotator (56 m) allows to have no focusing within the rotator. By introducing quadrupole triplets before and behind the rotator, which create a horizontal and vertical beam waist at about its center and match to the adjoining lattice, the transverse beam dimensions can be kept reasonably small (see Fig. 9). The absence of quadrupoles inside the mini rotator has two advantages: the positioning of the magnets does not need to be very accurate, except for keeping them correctly leveled transversely, and the spin matching of the optics, needed to maintain the spin transparency of the ring in the presence of the rotators, is much simpler. In fact, it has not been demonstrated that a ring with quadrupoles in the rotator could even be spin-matched at all.

The full variety of possible mini rotators has been investigated with a computer code [25]. Fig. 2 shows the result of the survey of rotators with a symmetric vertical bump. In this figure resembling a "weather map", the "isobars" connect rotator samples with equal figure of merit $L^2\Delta P/P$. The coordinate axes denote the spin rotation angles in the first two horizontally bending magnets next to the arcs of the ring. The (almost vertical) dash–dotted lines connect rotators replacing an integer number (1), (2), or (3) of normal arc magnets. The dotted line indicates a singularity in the off-energy correction using the vertical bump only. The two dashed lines connect rotators with vanishing tune shift. The figure shows that rotators with the highest figure of merit have nonvanishing spin tune shift and a very small energy range when tuning the energy with only the vertical beam bump.

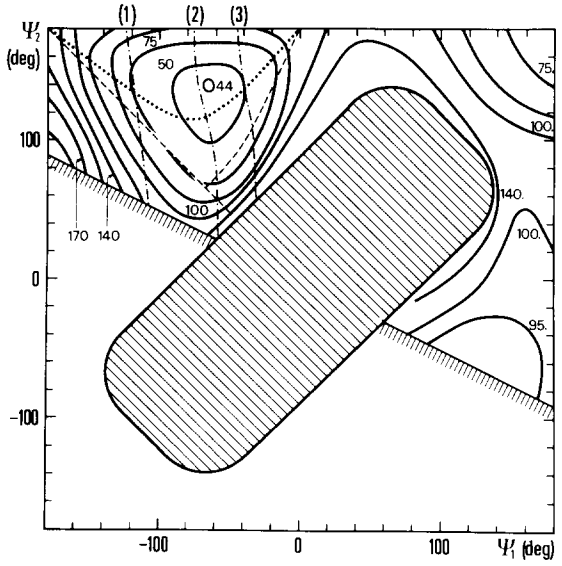

Fig. 2. Survey map of mini rotators with symmetric vertical beam bump.
ψ_1, ψ_2: spin rotation angles in the first two horizontally bending magnets next to the arcs of the ring.
Solid lines: curves for fixed figure of merit $L^2\Delta P/P$.
Other lines are explained in the text.
Hatched area: no solution.
mm limit of horizontally inward bending rotators.

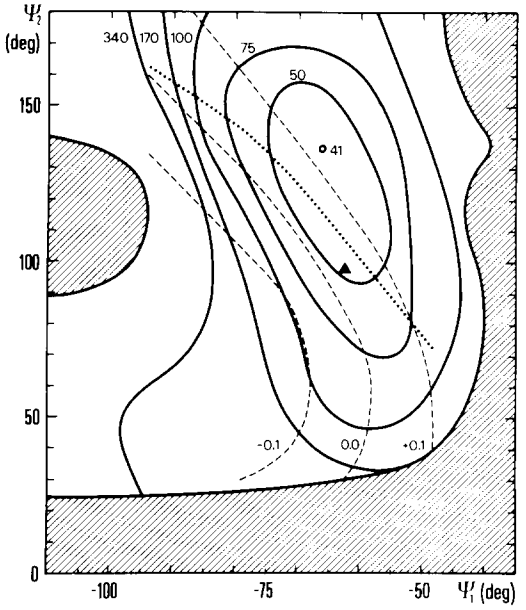

Fig. 3. Survey map of mini rotators with asymmetric vertical beam bump.
ψ_1, ψ_2: spin rotation angles in the first two horizontally bending magnets next to the arcs of the ring.
Solid lines: curves for fixed figure of merit $L^2\Delta P/P$.
Dashed lines: curves for fixed spin tune shift $(0, \pm 0.1)$.
Dotted line: curve for infinite off-energy correction using vertical beam bump only.
Hatched area: no real solution.
▲ proposed HERA mini rotator.

The survey has been extended to include rotators with nonsymmetric vertical bump [26], which allow to minimize the radiative excitation of vertical betatron oscillations in the rotator [11]. Fig. 3 shows the corresponding "weather map", where, at each point, the vertical beam bump geometry is adjusted for optimum polarization. The triangular mark indicates the proposed mini rotator which has been chosen as a com-

promise between a high degree of polarization and a small spin tune shift.

5. Chosen rotator parameters and properties

The rotator geometry finally chosen [12] is shown in fig. 4. The rotator is 56 m long and consists of three horizontal bending magnets H1, H2, H3, alternating with three vertical bends V1, V2, V3 which create the (asymmetric) vertical beam bump. As seen from the arc of the ring, the rotator proper is preceded by a bending magnet H4 (split in 2 parts) which, together with magnets H3 and H1, creates the horizontal beam bump needed for energy variation.

Table 1 gives the beam deflection and spin rotation angles in the rotator magnets at the reference energy ($E_0 = 29.79$ GeV, $\gamma a = 67.6$). Fig. 5 shows the magnitudes of the horizontal and vertical beam bumps versus energy. The maximum horizontal beam excursion (in H3) varies from -11 to $+8$ cm when going from 27 to 35 GeV. The vertical beam excursion varies between 20 and 22 cm in the same range.

For complete rotator action, there would be 3.2 mrad more bending in magnet H1. This bending has been transferrred to subsequent bends in magnets HTRA and HSEP, as explained in sect. 6. Together with these subsequent magnets, the rotator replaces exactly two standard bending magnets of the regular arc structure of the ring.

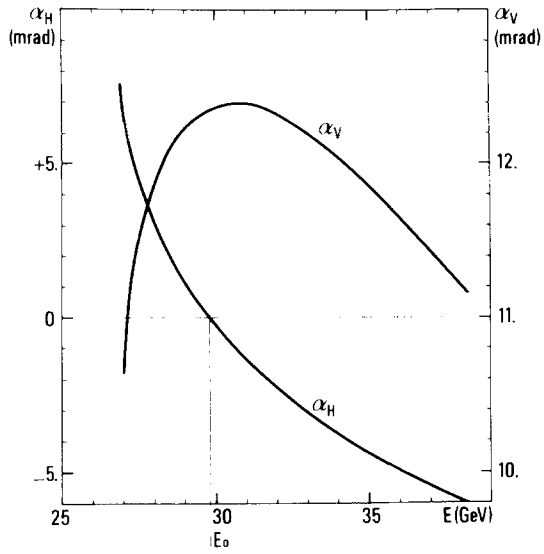

Fig. 5. Magnitude of horizontal and vertical beam bumps vs energy for the proposed HERA mini rotator.
α_H: difference of beam deflection in magnet H4 at energy E and at reference energy $E_0 = 29.79$ GeV.
α_V: vertical beam deflection in magnet V3.

Fig. 6 shows the maximum degree of polarization, given by the Sokolov–Ternov effect, the spin tune shift and the polarization time versus beam energy E. The observed reduction of the polarization, as compared to

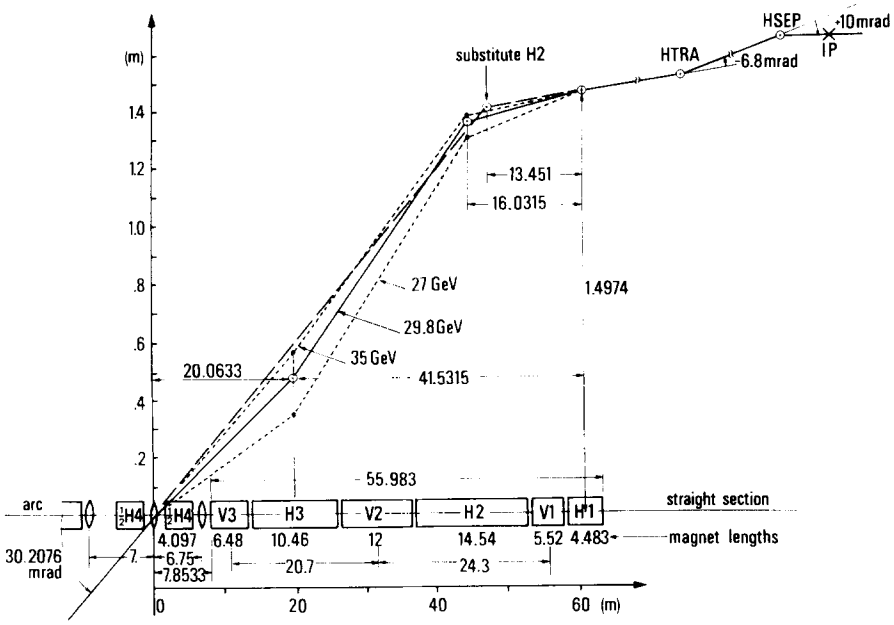

Fig. 4. Horizontal rotator geometry for three different energies: 27 GeV, 35 GeV and the reference energy $E_0 = 29.8$ GeV. The rotator substitute geometry is also shown (all lengths in m).

Table 1
Beam deflection ϕ and spin rotation α at the reference energy $E_0 = 29.788$ GeV, $\nu = 67.6$ ($\psi = \nu\phi$)

	H4	V3	H3	V2	H2	V1	H1
ϕ [mrad]	6.2855	$12.3555 = \alpha_v$	−11.0000	−22.8806	27.0076	10.5251	4.7145
ψ [deg]	–	47.8553	−42.6051	−88.6212	104.6058	40.7659	18.2602

the 92.376% value in a flat ring, scales approximately like E^{-3}.

6. Head-on collision with mini rotators incorporated

The mini rotator was originally designed for a collision geometry with crossing angle [1]. In that case, the spin leaves the rotator longitudinally and traverses the whole straight section length, with rf cavities and interaction region, in this orientation. When changing to head-on collision, with its unavoidable beam separating magnet just next to the interaction point, there was the problem how to incorporate the rotator in the presence of this magnet with its strong effect on spin rotation. The solution was to take away some bending from the last rotator magnet, H1, and transfer it into the separating magnet HSEP [3]. The horizontally oriented spin would then pass the rf straight section at an angular offset before being turned longitudinal in HSEP. This works indeed, but the dispersion generated in HSEP destroys the spin transparency of the straight section for synchrotron oscillations which, as it turns out, cannot be recovered without introducing another bend (see sect. 10). The translating magnet HTRA is inserted for this purpose in the rf section; it bends 6.8 mrad in the opposite direction and thus cancels the major part of the 10 mrad bend in HSEP. Only the balance of 3.2 mrad is now effectively transferred away from the rotator proper (see fig. 4).

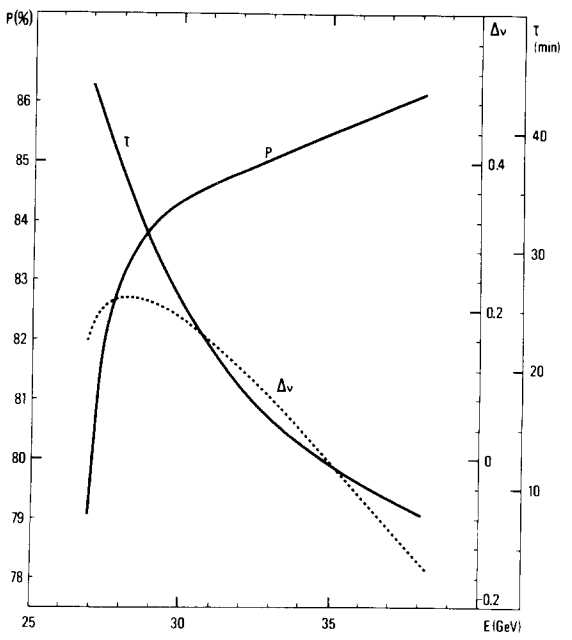

Fig. 6. Energy variation of Sokolov–Ternov polarization time τ, of equilibrium degree of polarization P and of spin tune shift $\Delta\nu$ in HERA equipped with four mini rotator pairs.

The ep collision geometry is shown in fig. 7. Starting along the same line from the interaction point, both the e and p orbits traverse the electron focusing quadrupole triplet and the separating magnet HSEP, where the electrons are bent by 10 mrad and separated by about this angle from the proton beam. The electrons then proceed through the rf section with magnet HTRA, through the rotator and into the arc, staying in the same ring plane throughout. The protons, after passing a proton focusing quadrupole doublet, go through a vertical translation before entering the periodic arc, where the proton ring is 81 cm on top of the electron ring.

In the collision geometry the rotator and straight section magnets, including HTRA and HSEP, replace in their overall bending exactly two of the normal arc magnets with a total deflection of 30.2 mrad, thus avoiding the construction of a special type of arc magnet. Only one rotator pair will be installed in HERA initially. This will allow to gain the necessary experience in tuning the machine for maximum transversal and longitudinal polarization, before rotator pairs will also be installed in the three other straight sections of the HERA ring. In these, the overall bend of the rotator will initially be replaced by a single rotator magnet H2, serving as a rotator substitute. With its bending angle of 27 mrad, H2 is tailored to serve this purpose in the collision geometry with magnets HTRA and HSEP in place.

The straight section WEST, however, which is located on the DESY site, will not have collision geometry initially. In order to facilitate injection and beam dump installation in this area, the magnets HTRA and HSEP will not be installed there, and neither will the vertical bends in the proton ring, such that the two beams will bypass each other sideways at a horizontal and vertical offset. In addition to the 27 mrad of the substitute magnet H2, another 3.2 mrad deflection is needed in this case to make up for the net deflection of the missing magnets HTRA and HSEP. It is suggested to

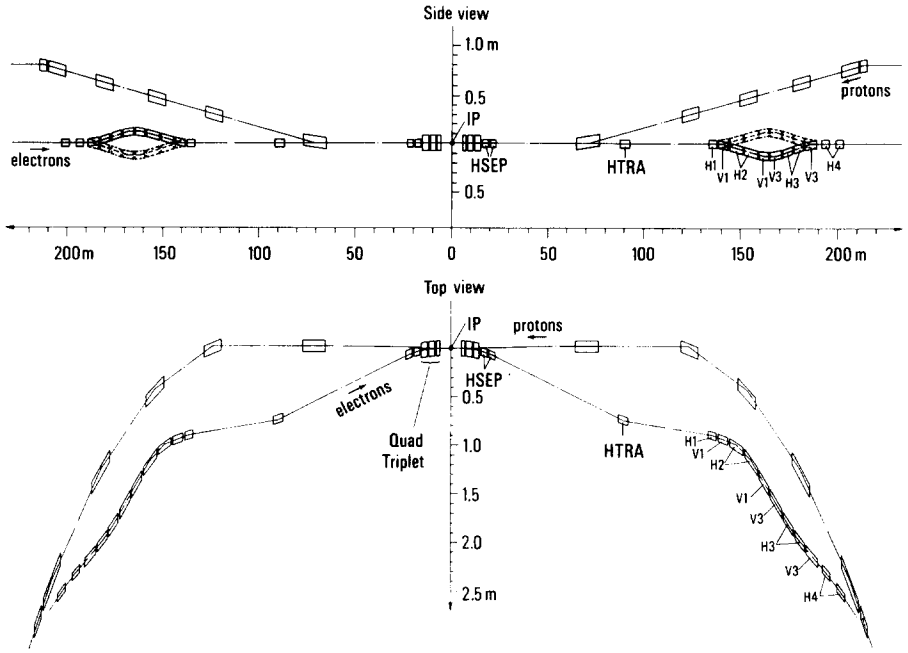

Fig. 7. HERA head-on ep collision geometry with mini spin rotators (bending magnets shown only).

install magnet H3 for this purpose. It will be weakly excited and can thus serve as a separating magnet for backscattered laser photons in a setup for measuring beam polarization [27]. The HERA straight section WEST can, at a later time, be rearranged for beam collision, if so required.

7. Technical rotator design aspects

Since the horizontal rotator magnets form part of the ring geometry that must stay unchanged during energy ramping, they must be excited strictly proportional to the main ring magnets. They are therefore powered in series with the main ring dipoles, which are C-type magnets with a "coil" consisting of a single $\sim 10 \times 10$ cm^2 aluminium bar. Similarly, all horizontal rotator magnets have a "bias coil" consisting of one or two thick aluminium bars which gives them exactly the beam deflections required at the reference energy of 29.788 GeV.

When changing the operating energy of the machine, the horizontal goemetry of the rotator will be changed by superimposing, within the rotator, the horizontal beam bump corresponding to the new energy and re-aligning the rotator magnets along this new beam line. The bump will be excited by special "bump coils" in rotator magnets H4, H3, and H1, wound of water-cooled copper conductor with 59, 50, and 38 turns, respectively. These numbers of turns and the magnet separations are chosen such that, when powered in series, the magnets will exactly produce the required closed beam bump. During energy ramping, the bump current will be varied proportional to the main ring current.

Spin rotation in the forward or backward direction is obtained by turning on the positive or negative vertical beam bump generated in magnets V3, V2, and V1. These magnets are again powered in series, antisymmetric to the interaction point within a rotator pair. In addition, they have correction coils which are also connected in series, but symmetric within the rotator pair such that they increase the vertical beam bump at one side of the interaction point while decreasing it at the other. This vertical bump correction is needed to adjust the overall spin transformation of the rotator pair (see sect. 8). For technical reasons, the long vertical magnet V2 is made up of one magnet V3 plus one magnet V1, so there are only two types of vertical magnets, having the same yoke and coils cross section but somewhat different lengths.

At the interaction quadrupole triplet, the bend HSEP deflects the electron beam about 10 mrad away from the much more energetic proton beam. Physically, only half of this deflection is done in a separate dipole magnet. The other half is obtained by slightly displacing the quadrupole magnets in the triplet horizontally, thus superimposing the required bending field on the focusing field. This effectively moves the bend up closer to the interaction point and thereby eases the problems caused by synchrotron radiation in that area.

The rotator magnet yokes are made of C-shaped laminations [28], fine-blanked out of 5 mm iron sheets, stacked and welded into a box of sheet steel [29] 5–15 mm thick, depending on magnet length. Similar to V2, also the longer horizontal magnets H3, H2 and HSEP are cut into two half-magnets for easing their support and coil construction. All copper coils are plane-wound coils that close around the upper and lower leg of the C-yoke, respectively.

The vertical beam bump requires a remotely controlled vertical motion of all rotator magnets between and including V3 and V1, with a maximum excursion of ± 22 cm from the median plane. Magnet motion must not be very precise, except for transverse levelling, but must be sufficiently synchronous in order to avoid undue stresses on coil and vacuum chamber connnections. Probably the cheapest and most reliable scheme will employ mechanical jacks driven by a common drive shaft.

8. Errors and corrections in the rotator pair

In order to avoid depolarization, it is necessary to have a vertical equilibrium spin direction, i.e. a vertical polarization in the arcs of the ring (see sect. 9). This means that the rotator pair between subsequent arcs must be so adjusted that a particle which enters the first rotator with vertical spin orientation will, after passing the straight section, leave the second rotator of the pair again with vertical spin orientation. The ideal rotator pair, of course, is designed to provide this exactly. In practice, however, the rotator magnets have errors, and it must be investigated what these errors do to the spin transformation, and how their effect can be corrected.

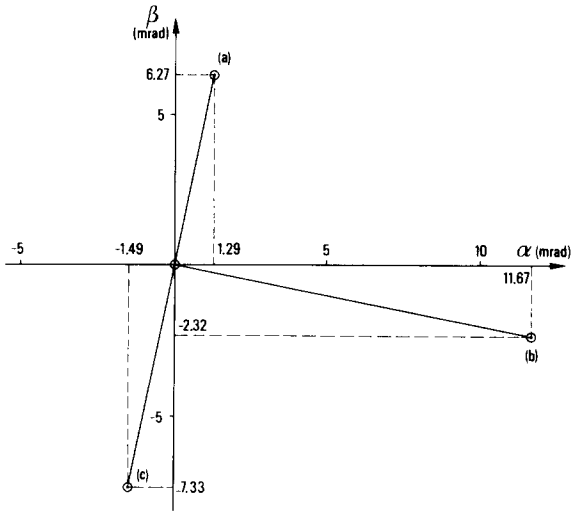

Fig. 8. Variation of spin transformation in the rotator pair by applying a pair of horizontal (a) or vertical (b) corrective beam bumps with a deflection of 0.1 mrad in the peak of the bumps. Point (c) is the error in spin transformation of the reference rotator pair for a machine energy offset of +0.2% from the reference energy. α and β are the longitudinal and transverse angular deviations of the outgoing spin direction from the vertical, respectively.

The spin transformation of the rotator pair can be characterized by a longitudinal angular deviation α and a transverse angular deviation β of the outgoing spin direction from the vertical, after having entered the pair with vertical orientation. These deviations have been determined [23] by subsequently applying to each magnet in the rotator pair a relative bending error of 1%; they turned out to be of the order of 10 mrad. On the other hand, the maximum deviation without significant effect on polarizaton is estimated to be of the order of 1 mrad [23]. Therefore, relative magnet errors must not exceed 10^{-3} which means that the rotator can be expected to be marginally operable even without correction.

However, there exist two very simple and effective orthogonal corrections for the spin transformation of the rotator pair [23,12], which will be incorporated. The first is the symmetric pair of horizontal beam bumps designed for energy variation. For an added deflection of 0.1 mrad in the peak of these bumps, the spin transformation, at reference energy, varies as given by point (a) in fig. 8, which shows the resulting angular deviations α and β. The beam bump, in this application, requires a slight correction by steeering coils for the small deflections due to the quadrupoles enclosed near one end, where the beam is slightly displaced by the bump correction. The second correction is done with correction coils in the vertical magnets which superpose on the antisymmetric main vertical bumps a pair of symmetric corrections that reduce the amplitude of one bump and increase the amplitude of the other. For an added deflection of 0.1 mrad in the peak of these bumps, the spin transformation, at reference energy, varies as given by point (b) in fig. 8.

It is seen that the two corrections are almost orthogonal and provide a beautiful handle for empirically optimizing the polarization in the presence of errors. With errors not only in the rotator, but also in the ring, the optimum adjustment will then not necessarily be obtained with an ideally compensated rotator pair, but rather with a setting that yields the best average vertical spin alignment in the arcs.

9. Spin diffusion by quantum emission

The energy jump caused by a quantum emission of synchrotron radiation in a bending magnet excites a synchrotron oscillation and also a horizontal or vertical betatron oscillation if the horizontal or vertical disper-

sion does not vanish in that magnet. In an ideally planar ring, only horizontal oscillations are produced and do not perturb the spin direction which, by the Sokolov–Ternov effect, is aligned along the vertical magnetic field. The ring is completely spin-transparent. However, in a real ring like HERA, with rotators and imperfections included, also vertical oscillations will be produced, and the equilibrium spin direction $\hat{\boldsymbol{n}}$ will not be vertical all around the ring. Then, the quantum excitation of vertical and horizontal oscillations will perturb the spin motion, and spin-transparency is destroyed. Within a few damping times following a quantum emission, the synchrotron and betatron oscillations will disappear again, and the particle will in general be left with a modified spin orientation. The result of successive random quantum emissions is a random diffusion of spins [30] away from the equilibrium direction. This spin diffusion competes with the Sokolov–Ternov polarizing effect and leads to an equilibrium degree of polarization which is lower than the Sokolov–Ternov limit of 92.4%.

The equilibrium spin direction $\hat{\boldsymbol{n}}(s)$, more explicitly, is the closed solution of the spin motion for an on-momentum particle circulating on the reference orbit; it transforms into itself after one revolution. In the arcs of the ring, this closed solution must be vertical in order to permit maximum radiative polarization in the field direction, but in the interaction regions, it is bent into the longitudinal by the mini rotators.

Induced by a quantum emission at the orbital position s, the change of spin direction away from the $\hat{\boldsymbol{n}}$-direction is proportional to the "spin–orbit coupling vector" $\boldsymbol{d}(s)$ which depends on the details of the optics and, in the general case, varies around the ring. The relative decrease in the equilibrium degree of polarization is proportional to the mean square of $\boldsymbol{d}$ all along the ring, according to the Derbenev–Kondratenko formula [30]:

$$p \simeq p_0 \frac{\int \frac{1}{\rho^3}(\hat{\boldsymbol{n}}\cdot\hat{\boldsymbol{h}})\,\mathrm{d}s}{\int \frac{1}{\rho^3}\left(1+\frac{11}{18}\boldsymbol{d}^2\right)\mathrm{d}s},$$

where $\hat{\boldsymbol{h}}$ is the unit vector parallel to the magnetic field.

However, by specially tailoring the optics, $\boldsymbol{d}(s)$ can be made small and the ring be made spin-transparent [14] at all bending magnets, and then the degree of polarization will approach the Sokolov–Ternov limit which, in a planar ring, is 92.4%. A detailed inspection of $\boldsymbol{d}(s)$ will reveal how this can be done.

Following Chao and Yokoya [31], the spin–orbit coupling vector $\boldsymbol{d}(s)$ can be written as:

$$\boldsymbol{d}(s) = \tfrac{1}{2}\mathrm{Im}\big[(\hat{\boldsymbol{m}}+\mathrm{i}\hat{\boldsymbol{l}})^* \times(\Delta_x+\Delta_{-x}+\Delta_z+\Delta_{-z}+\Delta_s+\Delta_{-s})\big],$$

where $\hat{\boldsymbol{m}}$ and $\hat{\boldsymbol{l}}$ are two orthogonal unit vectors, solutions of the spin motion and orthogonal to the closed solution. $\Delta_{\pm x,\pm z,\pm s}$ represent the contributions of the radial and vertical betatron and synchrotron oscillations respectively:

$$\Delta_{\pm x,z}(s) = \frac{(\gamma a+1)\,\mathrm{e}^{\mp \mathrm{i}\phi_{x,z}}}{\mathrm{e}^{2\mathrm{i}\pi(\nu\pm Q_{x,z})}-1} \times\frac{[-D\pm\mathrm{i}(\alpha D+\beta D')]_{x,z}}{\sqrt{\beta_{x,z}}} J_{\pm x,z}(s), \tag{2a}$$

$$\Delta_{\pm s}(s) = \frac{(\gamma a+1)\,\mathrm{e}^{\mp \mathrm{i}\phi_s}}{\mathrm{e}^{2\mathrm{i}\pi(\nu\pm Q_s)}-1} J_s(s), \tag{2b}$$

where D, D' are the dispersion and its slope and $\phi_{x,z,s}$ are the phases of betatron or synchrotron oscillations.

The first factor in Δ is a resonant factor which causes large depolarization whenever the beam energy is such that the spin tune ν approaches any of the values $\nu = n \pm Q_{x,z,s}$ (n integer).

Depolarization mainly occurs in the vicinity of these betatron or synchrotron sideband resonances.

The absolute value of the second factor (in brackets) in eq. (2a) is, when squared, just the emittance $\epsilon_{\mathrm{D}}(s)$ that can be locally attributed to the dispersion trajectory. This quantity is familiar from calculating the beam emittance. For vertical betatron oscillations, in absence of vertical orbit distortions, it differs from zero only in the mini rotators and can there be reduced by properly distributing the lengths of the horizontal magnets within the vertical beam bump [11] (see sect. 4).

But the real keys for obtaining high polarization are the spin-orbit coupling integrals that appear in eq. (2a, b) as the last factor $J_{x,z,s}(s)$:

$$J_{\pm x}(s) = \int_s^{s+c} (\hat{\boldsymbol{m}}+\mathrm{i}\hat{\boldsymbol{l}})\cdot\hat{\boldsymbol{e}}_z k\sqrt{\beta_x}\;\mathrm{e}^{\pm\mathrm{i}\phi_x}\,\mathrm{d}s', \tag{3a}$$

$$J_{\pm z}(s) = \int_s^{s+c} (\hat{\boldsymbol{m}}+\mathrm{i}\hat{\boldsymbol{l}})\cdot\hat{\boldsymbol{e}}_x k\sqrt{\beta_z}\;\mathrm{e}^{\pm\mathrm{i}\phi_z}\,\mathrm{d}s', \tag{3b}$$

$$J_s(s) = \int_s^{s+c} (\hat{\boldsymbol{m}}+\mathrm{i}\hat{\boldsymbol{l}})\cdot(\hat{\boldsymbol{e}}_z D_x+\hat{\boldsymbol{e}}_x D_z)k\,\mathrm{d}s', \tag{3c}$$

where c is the ring circumference, $k(s')$ is the quadrupole strength and $\hat{\boldsymbol{e}}_{x,z}$ the unit vector in the radial or vertical direction. For each type of oscillation, the corresponding integral is proportional to the effective spin rotation away from the equilibrium direction $\hat{\boldsymbol{n}}$ during one revolution around the ring, starting at the azimuth s of the quantum emission.

The scalar product $(\hat{\boldsymbol{m}}+\mathrm{i}\hat{\boldsymbol{l}})\cdot\hat{\boldsymbol{e}}_z$ vanishes in a planar ring without magnet errors, where $\hat{\boldsymbol{n}}(s')=\hat{\boldsymbol{e}}_z$ everywhere. In a real ring with vertical alignment errors of quadrupoles, however, the beam will be subjected to small vertical kicks which may cause the equilibrium spin to deviate from the vertical. In this case, the

coupling integrals J_x and J_s do not vanish and give a finite contribution from radial betatron and synchrotron oscillations to depolarization. In the absence of spin matching, this also, in general, occurs in those parts of an ideal ring where, between rotators, the equilibrium spin is designed to be in the horizontal plane.

Similarly, the vertical dispersion caused by vertical orbit distortions will give a finite contribution from vertical betatron and synchrotron oscillations to depolarization, since the coupling integrals J_z and J_s containing the scalar product $(\hat{\boldsymbol{m}} + \mathrm{i}\hat{\boldsymbol{l}}) \cdot \hat{\boldsymbol{e}}_x$ do not vanish in general. Again in a ring with rotators, the local vertical dispersion designed into the rotator has a similar effect if the ring is not carefully spin-matched.

10. Spin-transparent linear optics

As seen in the previous section, the rotators may partly destroy the spin transparency of the HERA electron ring by generating a nonvanishing spin-orbit coupling vector $\boldsymbol{d}(s)$ even in the ideal machine that has no magnet and alignment errors. This section will describe the "spin matching" of the HERA ring, i.e. the procedure for restoring its spin transparency in the absence of errors, while the next section will deal with "harmonic spin matching" as an additional tool for correcting the depolarizing effect of errors in the already spin-matched machine.

Spin matching, in general, consists of adjusting the linear optics of the machine such that the spin–orbit coupling integrals $J_{x,z,s}(s)$ as defined in eqs. (3a, b, c) vanish in every bending magnet. Applying it means that, in linear optics design, the familiar family of matching conditions for the optical functions (e.g. amplitudes and slopes of the horizontal and vertical dispersions and beta functions) is extended by including a number of spin-matching conditions of the type $J_{\pm x,z,s} = 0$, which are then simultaneously fulfilled by adjusting an increased number of optical parameters. This calls for an extension of the optical matching programs to include the spin-matching conditions. Such an extended program, called SPINOR, has been prepared by Hand [15] and successfully applied by Skuja [15] and Barber [17] in designing a spin-transparent HERA optics.

Essentially, one octant of the HERA ring consists of the following lattice sequence [32] (see also fig. 9):

- A periodic FODO arc with periodic optical functions.
- An end-region of the arc, where the strengths of about 12 quadrupoles are individually adjusted for simultaneous optical matching and spin matching. This region might be called a generalized dispersion suppressor.
- The rotator, preceded and followed by a quadrupole triplet. Over a length of about 60 m, there is no focusing within the rotator. In order to minimize beam size at the ends of this nonfocusing range, both amplitude functions should not be much over 60 m there.
- The rf channel: a nearly periodic "straight" FODO channel with rather strong focusing, loaded with rf accelerating units. Quadrupoles toward the ends are individually adjusted for matching. The channel contains the translating magnet HTRA.
- A drift space for beam growth, ending with the separating magnet HSEP.
- The interaction quadrupole triplet.
- The low-beta interaction region, 2×5.5 m long.

In the ideal ring, the equilibrium spin direction is vertical in the arc region up to the rotator. The arc region, therefore, does not contribute to the spin-orbit coupling integrals for horizontal oscillations, eq. (3a) and eq. (3c), first term. In the "straight" region between

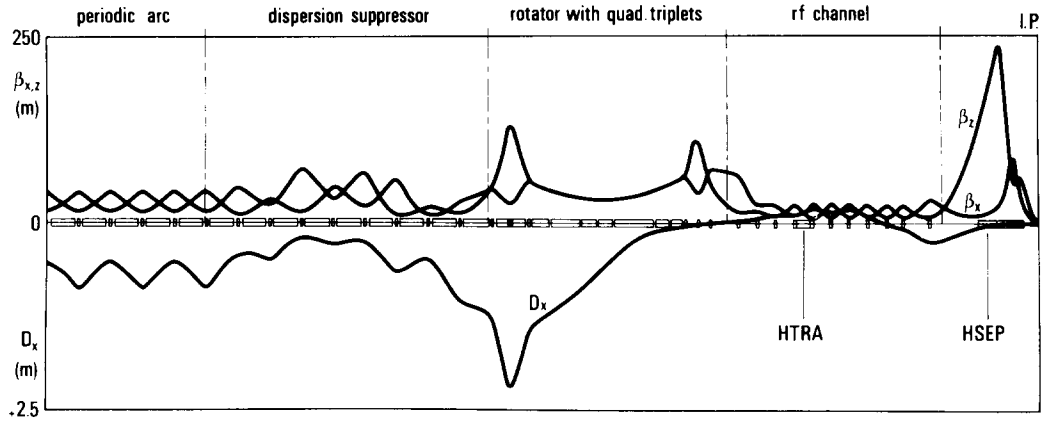

Fig. 9. Spin-matched electron optics for a HERA octant incorporating a rotator (D. Barber). Shown are the horizontal and vertical beta functions and the horizontal dispersion trajectory.

a pair of rotators, however, the vector $\hat{n}$ is in the horizontal plane and the coupling integrals (3a) and (3c), first term, will in general not vanish. They must therefore, by spin matching, be made to cancel. Since the lattice in the straight region is symmetric about the interaction point (I.P.), the spin-matching conditions for horizontal betatron and synchrotron oscillations may respectively be written

$$\int_{\text{I.P.}}^{\text{rotator}} k\sqrt{\beta_x}\,\cos\,\phi_x\,\mathrm{d}s = 0, \tag{4a}$$

$$\int_{\text{I.P.}}^{\text{rotator}} kD_x\,\mathrm{d}s = 0, \tag{4b}$$

with a betatron phase $\phi_x = 0$ at the interaction point. As the first integral is the change of slope of the cosine-like trajectory with respect to the I.P., eq. (4a) just requires that the slope of this trajectory be zero or, equivalently, $2\tan\phi_x = \beta_x'$ in the rotator. This is so because the spin rotation in the straight-section quadrupoles is proportional to the change of the trajectory slope.

The horizontal dispersion D_x in the straight region, being identically zero at the I.P., is generated by the separating magnet HSEP next to the interaction triplet and, from there on, would traverse the whole region as a particular betatron trajectory if there were no further bends. This trajectory would have a sine-like as well as a cosine-like constituent symmetric to the I.P., and eq. (4b) would require in addition to eq. (4a)

$$\int_{\text{I.P.}}^{\text{rotator}} k\sqrt{\beta_x}\,\sin\,\phi_x\,\mathrm{d}s = 0, \tag{4c}$$

which is incompatible with eq. (4a) and cannot simultaneously be satisfied [3]. Therefore, we introduced into the rf channel the translating magnet HTRA which adds another contribution to the integral (4b) and makes it vanish [16].

Both matching conditions (4a) and (4b) are of purely optical nature and do not depend on energy. They make the ring spin-transparent for horizontal oscillations generated by radiation in all bending magnets in the arc and in the rotators. In principle, horizontal betatron oscillations are generated also in the straight region in magnets HTRA and HSEP, where spin transparency is not established by eq. (4a), but radiation is so weak and dispersion so small in these magnets that their effect on spin diffusion might be ignored.

For vertical oscillations, the situation is different. In the ideal uncoupled machine, a vertical dispersion exists only in the rotators, and only there can vertical betatron oscillations be excited by radiation. Thus, the machine must be made spin-transparent at the rotators only. For vertical synchrotron oscillations, no matching condition arises since there are no quadrupoles in the rotator as being the only region with vertical dispersion, and the second term in the integral (3c) gives no contribution to J_s.

For establishing the spin transparency for vertical oscillations at all rotators, the straight region as well as the arc region must be made spin-transparent. For the straight region, employing its symmetry again, this means that

$$\int_{\text{I.P.}}^{\text{rotator}} (\hat{n}\cdot\hat{s})\,k\sqrt{\beta_z}\,\cos\,\phi_z\,\mathrm{d}s = 0, \tag{4d}$$

according to eq. (3b), with $\phi_z = 0$ at the I.P. and $(\hat{n}\cdot\hat{s})$ being the longitudinal component of the equilibrium spin direction $\hat{n}$.

Spin matching for the arc is more elaborate. If the arc is not symmetric about its center line (C.L.), four matching conditions must be satisfied, as given by eq. (3b):

$$\int_{(\text{arc})} \begin{Bmatrix} \cos\,\psi \\ \sin\,\psi \end{Bmatrix} k\sqrt{\beta_z} \begin{Bmatrix} \cos\,\phi_z \\ \sin\,\phi_z \end{Bmatrix} \mathrm{d}s = 0, \tag{4e}$$

where $\psi(s)$ is the spin precession angle. If the arc region is symmetric, this simplifies to

$$\int_{\text{arcC.L.}}^{\text{rotator}} \begin{Bmatrix} \cos\,\psi\,\cos\,\phi_z \\ \sin\,\psi\,\sin\,\phi_z \end{Bmatrix} k\sqrt{\beta_z}\,\mathrm{d}s = 0, \tag{4f}$$

with $\psi = \phi_z = 0$ at the arc center line.

In contrast to the conditions (4a) and (4b) for horizontal matching, the vertical matching conditions (4d) and (4e, f) are not of a purely optical nature; via the spin precession angle ψ they depend explicitly on energy and must be rematched whenever the operating energy of the machine is changed.

A spin-transparent optics as matched by Barber [17] for a HERA octant incorporating a rotator is shown in fig. 9. The degree of polarization calculated for this ring with three rotator pairs and no errors is 85% at 35 GeV.

11. Harmonic spin matching

Even if exact matching is achieved for the mini rotators, as shown in the previous section, the degree of polarization is still expected to be lower than allowed by the Sokolov–Ternov effect due to ring imperfections (magnet errors and misalignments). These imperfections are responsible for small deviations of the equilibrium spin direction from the vertical in the arcs. Consequently radial betatron and synchrotron depolarizing resonances are excited as explained in sect. 9. Moreover these imperfections produce a vertical dispersion which excites vertical betatron resonances and contributes to the spin–orbit coupling integral (3c) for synchrotron oscillations. Finally, the radial dispersion is modified by imperfections. In the "straight" regions between rotators, where the spin is horizontal, this radial dispersion error causes spin rotation for off-momentum particles and thus contributes to the spin–orbit coupling integral (3c) for synchrotron oscillations. This disappears when the mini rotators are turned off.

Quite generally the amount of depolarization due to imperfections changes when mini rotators are turned on or off. The reason is that the kicks given to the spin in the straight regions between rotators depend on the spin orientation, which is vertical when the mini rotators are "off", and horizontal when they are "on".

Depolarization due to imperfections is expected to be important for HERA, and larger than in the PETRA storage ring, as the spin rotation errors are proportional to beam energy. A high degree of polarization can only be obtained by greatly reducing this depolarization.

In principle it could be achieved by making the ring spin-transparent for any type of oscillation excited by quantum emission at whatever point in the ring. The procedure would be similar to what has been done for the mini rotators. It would require one to cancel out the spin–orbit coupling integrals $J_{\pm x,z,s}$ everywhere, i.e. for each bending magnet in the ring. This is in fact impracticable as spin-matching conditions (ten for each magnet) are too numerous even when the periodicity and symmetry properties of the ring are considered. There are not enough degrees of freedom to fulfil simultaneously all these conditions.

However, the largest contribution to depolarization comes from the excitation of the few depolarizing resonances closest to the spin tune. It is enough to compensate these nearby resonances [19,20], as was done experimentally at PETRA [18] by using a small number of vertical orbit corrections (two per resonance).

The procedure for compensating a particular depolarizing resonance is called "harmonic spin matching" and must be discriminated from the usual spin matching which cancels out all resonances simultaneously and which achieves complete spin transparency in a ring without errors. Effectively the strength of a particular depolarizing resonance is obtained by a harmonic analysis of the corresponding spin–orbit coupling integral, which can be written (see eqs. (3a, b, c)):

$$J_y = \int_s^{s+c} \omega_y(s')\,\mathrm{d}s' \quad y = \pm x,\ \pm z,\ s \tag{5a}$$

where the complex integrand $\omega_y(s')$ gives the components along the $\hat{\boldsymbol{l}}$ and $\hat{\boldsymbol{m}}$ directions of the perturbing spin rotation vector as a function of the azimuth s. The integrand $\omega_y(s)$ has a $2\pi(\nu \pm Q_y)$ phase advance per turn and can be analysed in frequency as:

$$\omega_y(s) = \sum_p \omega_{p,y}\, \mathrm{e}^{2\mathrm{i}\pi(\nu - p \pm Q_y)s/c} \quad (p \text{ integer}) \tag{5b}$$

with

$$\omega_{p,y} = \int_0^c \omega_y(s)\, \mathrm{e}^{-2\mathrm{i}\pi(\nu - p \pm Q_y)s/c}\, \mathrm{d}s/c. \tag{5c}$$

The spin–orbit coupling integral J_y is large only in the vicinity of each $\nu = p \pm Q_y$ resonance. On top of such a resonance the perturbing spin rotation vector stays in phase with the normal spin precession, and J_y is proportional to the coefficient $\omega_{p,y}$ which gives the strength of this resonance. Harmonic spin matching consists of canceling $\omega_{p,y}$ for each resonance to be compensated.

In fact $\omega_{p,y}$ varies with energy slowly. Its variation only comes from the fact that, in the integral $\omega_{p,y}$ (eq. (5c)), the phase advance is uniform for the exponential, while the phase of ω_y changes only in bending magnets, leading to

$$\frac{\mathrm{d}\omega_{p,y}}{\omega_{p,y}} \simeq \pi\left(\frac{R}{\rho} - 1\right)\frac{\mathrm{d}\gamma}{\gamma},$$

i.e.

$$\frac{\mathrm{d}\omega_{p,y}}{\omega_{p,y}} \simeq 2\frac{\mathrm{d}\gamma}{\gamma} \quad \text{for HERA,}$$

with a bending radius $\rho = 608$ m and an average radius $R = 1008$ m. Up to a few percent it suffices, in the case of HERA, to cancel out the coefficient $\omega_{p,y}$ on the top of the corresponding resonance, as the nearby resonances differ from the operating point by less than 220 MeV in energy, as compared to a beam energy of 27–35 GeV. On the top of the resonance, the exponential in $\omega_{p,y}$ becomes unity; then $\omega_{p,y}$ is identical to the spin–orbit coupling integral J_y, which is independent of the origin since its integrand then is periodic.

Firstly, let us consider the vertical betatron resonances, driven by an unwanted vertical dispersion. In the spin matching integral (3b), the integrand

$$\omega_z(s) = (\hat{\boldsymbol{m}} + \mathrm{i}\hat{\boldsymbol{l}}) \cdot \hat{\boldsymbol{e}}_x k\sqrt{\beta_z}\ \mathrm{e}^{\pm \mathrm{i}\phi_z}$$

does not, to zero order, depend on imperfections, and thus has the superperiodicity of the ring. In a fourfold symmetric ring, for example, the main vertical betatron resonances are separated by 4 units (the order p is a multiple of 4), and it is advantageous to choose the operating point such that the spin tune is roughly midway, i.e. separated by about 2 units from the main vertical betatron resonances. Other vertical resonances ($p = 4n + 1, 4n + 2, 4n + 3$) will be weaker. Compensation, i.e. harmonic spin matching for vertical betatron oscillations, is then done by suitably adjusting the quadrupole strengths in the ring such that the matching integral vanishes at the nearby resonances [20].

Secondly, we consider the radial betatron resonances and the synchrotron resonances. They are driven by the horizontal dispersion in conjunction with a deviation $\mathrm{d}\hat{\boldsymbol{n}}$ of the equilibrium spin direction $\hat{\boldsymbol{n}}$ away from the vertical and, for the synchrotron resonances, also by an unwanted vertical dispersion D_z as well as by a radial dispersion error ΔD_x in the interaction regions with mini rotators turned on. Vertical dipole correctors can modify both the direction $\hat{\boldsymbol{n}}$ and the dispersions D_z and ΔD_x. The spin matching integrals (3a) and (3c)

$$\int_0^c (\hat{\boldsymbol{m}} + \mathrm{i}\hat{\boldsymbol{l}}) \cdot \hat{\boldsymbol{e}}_z k\sqrt{\beta_x}\ \mathrm{e}^{\pm \mathrm{i}\phi_x}\, \mathrm{d}s'$$

$$\int_0^c (\hat{\boldsymbol{m}} + \mathrm{i}\hat{\boldsymbol{l}}) \cdot (\hat{\boldsymbol{e}}_z D_x + \hat{\boldsymbol{e}}_x D_z) k \, \mathrm{d}s',$$

calculated on top of the resonances to be considered, are then sensitive to such correctors. By inverting the linear mapping between the correctors and these integrals, one can find a set of corrector conbinations which act on each integral separately. At a given energy, this linear mapping is completely determined once the unperturbed ring optics is known. Experimentally, by trial and error one will then find the amplitude of each corrector combination which optimizes the polarization. This procedure of simultaneous harmonic spin matching for horizontal betatron oscillations and for synchrotron oscillations [33] is just an extension, in principle more efficient, of the procedure of canceling certain harmonics of the deviation $\mathrm{d}\hat{\boldsymbol{n}}$, as successfully applied at PETRA. An almost equivalent procedure for optimizing depolarization is to correct the most important harmonics of the spin–orbit coupling vector $\boldsymbol{d}(s)$ itself, as investigated by Mane [34].

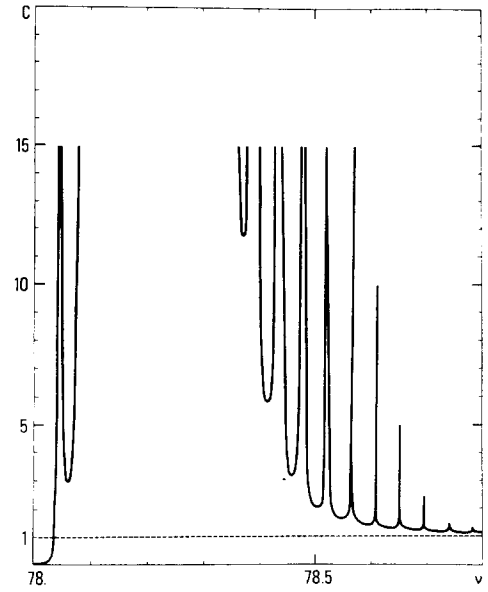

Fig. 10. Depolarization enhancement factor C as a function of spin tune in HERA near 35 GeV.

12. Depolarization enhancement by energy spread

Depolarization by spin diffusion due to quantum emission was, in preceding sections, considered only as a linear effect in the amplitudes of oscillation. Beam energy spread and synchrotron oscillation amplitudes, however, become large at high energies, and the associated nonlinear effects are expected to become important. In HERA, the relative standard deviation σ_E/E of energy spread is 0.95×10^{-3} at 27.5 GeV and increases linearly with energy. So the absolute energy spread increases quadratically and its standard deviation reaches 42 MeV at 35 GeV. On the other hand, the spacing between depolarizing resonances does not change with energy and, in an electron ring, each particular type of resonance occurs repeatedly with a constant separation of 440 MeV. Particles with sufficiently large energy deviation, i.e. with large synchrotron amplitude, may then approach the resonance energy even if the central beam energy is set as far as possible away from nearby resonances. Larger depolarization than expected for small oscillations from linear theory can then occur.

However, this picture of a particle approaching a resonance is not very consistent as it mixes the time domain and the frequency domain. A more correct way of considering this energy spread effect is to take into account the frequency modulation of spin precession produced by synchrotron oscillations, as spin tune is proportional to energy. This situation is very similar to the well-known effect of frequency modulation in rf waves. It leads to the appearance of satellites around the central frequency. Similarly for the spin motion, synchrotron satellites are generated around any depolarizing resonance. These satellites are regularly spaced by the synchrotron tune Q_s. If the energy spread is sufficiently large, involving large synchrotron amplitudes, then several satellites are excited and the energy range in which depolarization by a particular resonance occurs is widened. This is equivalent to saying that particles with large energy spread are approaching resonance.

This nonlinear depolarization effect has been studied analytically by several authors [35–39]. The result is expressed in terms of depolarization enhancement for each resonance. The contribution of each resonance to the square average of the spin–orbit coupling vector $\boldsymbol{d}(s)$ is multiplied by an enhancement factor C which becomes very large on the top of the excited synchrotron satellites. The number of excited satellites increases with the product $\nu/Q_s \cdot (\sigma_E/E)$ which scales nearly quadratically with energy.

Fig. 10 shows, as an example, the enhancement factor of the resonance $\nu = 78$, exhibiting for HERA near 35 GeV the large number (≈ 12) of excited synchrotron satellites [21]. Setting the operating point in the middle between two satellites and near a half-integer spin tune, the enhancement factor is about a factor 2. It means that, in HERA at 35 GeV, one has to be two times more efficient in order to get the same polarization as in the case of smaller energy spread. Also, the choice of the operating point becomes more delicate. At lower energies the number of excited satellites is lower and this problem becomes less serious [40].

Acknowledgments

Many colleagues of the HERA group have contributed to the final lattice design. In particular, we are indebted to D. Barber for his persistent efforts in tackling and solving the matching problems, and wish to thank J. Kewisch, S.R. Mane and G.-A. Voss for fruitful discussion.

References

[1] HERA proposal, DESY HERA 81/10.
[2] A. Piwinski, Proc. Particle Accelerator Conf., Vancouver (1985).
[3] K. Steffen, DESY HERA 84/09 (1984).
[4] K. Steffen, Proc. 6th Int. Symp. on High energy spin physics, Marseille (1984), J. Phys. Coll. C2, suppl. no. 2, 46 (1985) 601 and DESY HERA 84/27 (1984).
[5] D. Barber, R. Brinkmann, R. Kose, J. Rossbach, K. Steffen and F. Willeke, Proc. Particle Accelerator Conf., Vancouver (1985) and DESY M-85-08.
[6] A.A. Sokolov and I.M. Ternov, Sov. Phys. Doklady 8 (1964) 1203.
[7] K. Steffen, DESY HERA 83/06 (1983).
[8] D. Barber, J. Kewisch, G. Ripken, R. Rossmanith and R. Schmidt, DESY 84-102 (1984).
[9] K. Steffen, DESY HERA 83/09 (1983).
[10] J. Buon and K. Steffen, DESY HERA 84/25 (1984).
[11] K. Steffen, DESY HERA 85/07 (1985).
[12] J. Buon and K. Steffen, DESY HERA 85/09 (1985).
[13] J. Buon, LAL NI/07-81 and LAL/RT/81-08, Orsay (1981).
[14] A. Chao and K. Yokoya, KEK 81-7 (1981), TRISTAN (A).
[15] L. Hand and A. Skuja, DESY HERA 85/18 (1985).
[16] D. Barber and K. Steffen, private communication (1984).
[17] D. Barber, private communication (1985).
[18] H. Bremer, J. Kewisch, H. Lewin, H. Mais, R. Rossmanith and R. Schmidt, DESY 82-026 (1982).
[19] K. Steffen, DESY HERA 82-02 (1982).
[20] S. Holmes and K. Steffen, CBN 82-10, Cornell, Newman Lab. (1982).
[21] J. Buon, DESY HERA 85-08 (1985).
[22] K. Steffen, DESY PET 78/11 (1978).
[23] K. Steffen, DESY HERA 84/03 (1984).
[24] J. Buon, in: Proc. of ref. [4], p. 631 (1985) and LAL/RT/84-04, Orsay (1984).
[25] J. Buon, LAL/RT/83-10, Orsay (1983) and DESY HERA 83/20 (1983).
[26] J. Buon, DESY HERA 84/11 (1984).
[27] T. Limberg, private communication (1985).
[28] K. Steffen, DESY HERA 85/19 (1985).
[29] H. Kaiser and H. Wümpelmann, DESY M-80/01 (1980).
[30] Ya.S. Derbenev and A.M. Kondratenko, Sov. Phys. JETP 37 (1973) 968.
[31] A. Chao and K. Yokoya, Résumé Workshop on Polarized electron acceleration and storage, DESY M-82/09 (1982) p. K9 and p. R19.
[32] K. Steffen, DESY HERA 83/16 (1983).
[33] J. Buon and S.R. Mane, private communication (1985).
[34] S.R. Mane, private communication (1985).
[35] Ya.S. Derbenev, A.M. Kondratenko and A.N. Skrinsky, Part. Accel. 9 (1979) 247.
[36] C. Biscari and J. Buon, LAL NI/40-81 (1981).
[37] J. Buon, LAL/RT/83-02 (1983).
[38] C. Biscari, J. Buon and B. Montague, Nuovo Cimento 81E (1984) 128 and CERN/LEP-TH/83-8 (1983).
[39] K. Yokoya, unpublished KEK report (1982).
[40] J. Buon, DESY HERA 83-14 (1983).